

# CALCULATION OF SNOW AVALANCHE RUNOUT DISTANCE

by

S. Bakkehøi, U. Domaas and K. Lied

(Norges Geotekniske Institutt, P.O. Box 40 Tåsen, Oslo 8, Norway)

## ABSTRACT

Distance of maximum avalanche runout is calculated by four topographical factors. An empirical equation found by regression analysis of 206 avalanches is used to predict the maximum runout distance in terms of average gradient of the avalanche path (angle  $\alpha$ ). The correlation coefficient  $R = 0.92$ , and the standard deviation of the residuals  $SD = 2.3^\circ$ .

The avalanche paths are further classified into different categories depending on confinement of the path, average inclination of the track  $\beta$ , curvature of the path  $y''$ , vertical displacement  $Y$ , and inclination of rupture zone  $\theta$ . The degree of confinement is found to have no significant effect on the runout distance expressed by  $\alpha$ . Best prediction of runout distance is found by a classification based on  $\beta$  and  $Y$ . For avalanches with  $\beta < 30^\circ$  and  $Y > 900$  m,  $R = 0.90$  and  $SD = 1.02^\circ$ .

The population of avalanches is applied to a numerical/dynamical model presented by Perla and others (1980). Different values for the friction constants  $\mu$  and  $M/DY$  are computed, based on the observed extent of the avalanches. The computations are supplied by velocity measurements  $v$  from a test avalanche where  $Y \approx 1\ 000$  m, and  $v_{max} \approx 60$  m s<sup>-1</sup>. The best fitted values are  $\mu = 0.25$  and  $M/DY = 0.5$ , which gives  $R = 0.83$  and  $SD = 3.5^\circ$ .

## 1. INTRODUCTION

Evaluation of the maximum runout distance of snow avalanches is one of the most important problems in avalanche zoning. It is also one of the most difficult and controversial subjects in avalanche research. This is especially true in avalanche-prone districts where there may be a need for housing, so that calculation of maximum runout distance has many implications concerning possible future accidents and damage.

Models that will predict avalanche runout distance are therefore much in need. Such models should be based on a small number of parameters. These parameters should be as objective as possible, and not be based on subjective judgment from the various avalanche experts handling the problem.

The purpose of this paper is to study extreme avalanche runout distance based on (1) topographic parameters from about 200 avalanches, (2) calculation of runout distance from the same collection of avalanches based on a numerical/dynamical model, and (3) combination of the two models.

## 2. RUNOUT DISTANCE BASED ON TOPOGRAPHICAL PARAMETERS

Evaluation of maximum runout distance of avalanches based on topographical parameters is

described by Lied and Bakkehøi (1980). These parameters could be easily identified on a topographic map, so that the subjective judgment of the numerical values belonging to the different parameters could be neglected. In the present work, the number of avalanches studied is increased from 111 to 206; the maximum extent of all these is known and listed in Table I. The avalanches chosen for this study have quite different paths, ranging from steep slopes, with an abrupt transition to the valley floor, to long, gently inclined paths with a gradual transition from track to runout zone. The extent of rupture area and degree of confinement in the path varies greatly.

The parameters which may be used to evaluate maximum avalanche runout are the average gradient of the avalanche path  $\alpha$ , the average inclination of the avalanche track  $\beta$ , the inclination of starting zone  $\theta$  (measured on map), the second derivative  $y''$  of the slope function  $y = ax^2 + bx + c$ , the vertical drop  $Y$ , and the height  $H$  from the starting point to the vertex of the parabola. These parameters are illustrated in Figure 1, and are derived as follows. The angle  $\alpha$ , which describes the total reach of the avalanche, is determined on the path profile by the line connecting the end points for the largest known event. The angle  $\beta$  is determined by the line connecting the top point, and the point on the profile where the slope angle is  $10^\circ$ . The reason for using this line, or angle, is to generate a simple description of the main inclination of the track. Slope gradient values around  $10^\circ$  are thought to represent the transition zone between the track and the runout zone for big, dry avalanches (de Quervain 1972, Buser and Frutiger 1980).

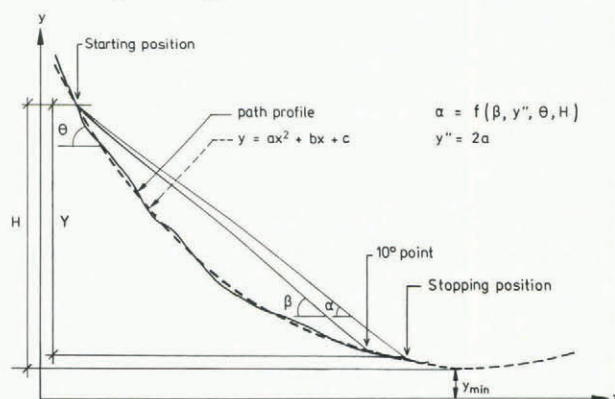


Fig.1. Topographical variables for the calculation of  $\alpha$ .

TABLE I. LIST OF AVALANCHES  
(for explanation of column headings, see text)

Ava-lanche	$\alpha$	$\beta$	$\theta$	H	$y''$	Ava-lanche	$\alpha$	$\beta$	$\theta$	H	$y''$	Ava-lanche	$\alpha$	$\beta$	$\theta$	H	$y''$
1	31.0	32.0	50.0	605	0.82E-03	70	40.5	44.0	53.0	718	0.18E-02	138	25.0	29.0	35.0	1000	0.28E-03
2	26.0	31.0	40.0	698	0.64E-03	71	39.0	41.0	41.5	555	0.17E-02	139	28.0	30.0	45.0	1000	0.52E-03
3	33.0	38.0	47.0	968	0.92E-03	72	35.0	36.5	39.0	620	0.86E-03	140	31.0	34.0	45.0	670	0.11E-02
4	36.0	40.0	49.0	711	0.13E-02	73	36.0	34.0	41.5	410	0.92E-03	141	31.0	34.0	35.0	550	0.86E-03
5	27.0	30.0	38.0	342	0.10E-02	74	35.0	32.0	39.0	435	0.86E-03	142	30.0	35.0	40.0	590	0.11E-02
6	38.0	43.0	55.0	582	0.16E-02	75	33.5	32.5	39.0	475	0.84E-03	143	30.0	35.0	45.0	850	0.66E-03
7	31.0	35.0	50.0	958	0.66E-03	76	30.0	34.0	39.0	610	0.62E-03	144	41.0	38.0	55.0	650	0.20E-02
8	28.0	32.0	45.0	528	0.90E-03	77	36.0	35.0	53.5	565	0.90E-03	145	35.0	37.0	40.0	1110	0.40E-03
9	30.0	34.0	48.0	515	0.11E-02	78	26.0	28.0	45.0	550	0.64E-03	146	34.0	36.0	36.0	1110	0.18E-03
10	29.0	33.0	41.0	487	0.11E-02	79	25.5	28.0	36.0	635	0.54E-03	147	43.0	34.0	42.0	1105	0.80E-03
11	28.0	32.0	36.0	491	0.98E-03	80	24.0	25.0	36.0	540	0.38E-03	148	40.0	42.0	45.0	1225	0.74E-03
12	28.0	34.0	39.0	640	0.90E-03	81	19.0	22.0	39.0	455	0.88E-03	149	32.0	43.0	32.0	1275	0.48E-03
13	26.0	33.0	38.0	612	0.78E-03	82	27.0	27.5	45.0	445	0.76E-03	150	39.0	42.0	27.0	1275	0.80E-03
14	29.0	33.0	40.0	480	0.12E-02	83	25.0	27.0	29.0	625	0.38E-03	151	39.0	40.0	27.0	1275	0.84E-03
15	35.0	35.0	35.0	394	0.18E-02	84	23.5	27.5	33.0	690	0.38E-03	152	39.0	41.0	54.0	1220	0.86E-03
16	37.0	39.0	47.0	932	0.72E-03	85	26.5	33.0	44.0	575	0.64E-03	153	38.0	42.0	39.0	1250	0.78E-03
17	35.0	40.0	42.0	1125	0.90E-03	86	25.0	26.0	39.0	485	0.50E-03	154	37.0	42.0	39.0	1220	0.76E-03
18	23.0	29.0	37.0	570	0.50E-03	87	24.0	30.0	35.0	725	0.76E-03	155	35.0	40.0	40.0	1210	0.72E-03
19	33.0	39.0	51.0	1131	0.78E-03	88	24.0	27.0	40.0	860	0.32E-03	156	37.0	45.0	40.0	1170	0.70E-03
20	31.0	35.0	40.0	938	0.68E-03	89	23.0	27.0	40.0	825	0.36E-03	157	39.0	46.0	49.0	950	0.10E-02
21	34.0	36.0	52.0	1015	0.72E-03	90	23.0	26.0	40.0	850	0.36E-03	158	38.0	45.0	49.0	950	0.11E-02
22	32.0	38.0	43.0	1110	0.78E-03	91	22.0	23.0	45.0	730	0.32E-03	159	41.0	44.0	54.0	950	0.12E-02
23	20.0	21.0	36.0	831	0.17E-03	92	22.0	25.0	38.0	775	0.24E-03	160	40.0	41.0	40.0	1230	0.42E-03
24	27.0	29.0	38.0	682	0.36E-03	93	26.0	27.0	39.0	750	0.34E-03	161	38.0	43.0	40.0	985	0.74E-03
25	33.0	40.0	48.0	1035	0.10E-02	94	28.0	30.0	44.0	750	0.64E-03	162	38.0	39.0	45.0	1155	0.68E-03
26	26.0	32.0	51.0	830	0.62E-03	95	26.0	34.0	50.0	640	0.82E-03	163	37.0	40.0	31.0	1150	0.62E-03
27	24.0	32.0	37.0	1175	0.40E-03	96	34.0	37.0	40.0	650	0.12E-02	164	37.0	40.0	31.0	1000	0.64E-03
28	34.0	34.0	52.0	608	0.96E-03	97	42.0	40.0	55.0	675	0.13E-02	165	38.0	38.0	29.0	990	0.58E-03
29	30.0	31.0	45.0	1086	0.42E-03	98	35.0	33.0	50.0	530	0.11E-02	166	40.0	39.0	39.0	945	0.40E-03
30	34.0	35.0	52.0	1175	0.46E-03	99	32.0	33.0	39.0	650	0.15E-02	167	35.0	38.0	31.0	850	0.24E-03
31	33.0	35.0	46.0	1153	0.54E-03	100	33.0	36.0	39.0	615	0.13E-02	168	38.0	35.0	31.0	765	0.78E-03
32	29.0	32.0	45.0	767	0.62E-03	101	34.0	36.0	40.0	600	0.13E-02	169	38.0	36.0	39.0	640	0.12E-02
33	29.0	31.0	45.0	840	0.52E-03	102	33.0	37.0	45.0	600	0.16E-02	170	40.0	43.0	45.0	1040	0.84E-03
34	28.0	30.0	40.0	1539	0.20E-03	103	25.0	29.0	30.0	700	0.40E-03	171	35.0	37.0	40.0	1410	0.40E-03
35	27.0	30.0	40.0	1466	0.22E-03	104	32.0	37.0	45.0	800	0.13E-02	172	42.0	45.0	45.0	825	0.11E-02
36	27.0	30.0	40.0	1475	0.22E-03	105	31.0	36.0	51.0	600	0.14E-02	173	49.0	51.0	45.0	1115	0.92E-03
37	30.0	32.0	40.0	1239	0.34E-03	106	31.0	36.0	45.0	560	0.11E-02	174	49.0	51.0	45.0	1220	0.12E-02
38	26.0	33.0	42.0	1306	0.38E-03	107	26.0	32.0	39.0	900	0.56E-03	175	49.0	48.0	45.0	1115	0.12E-02
39	21.0	26.0	50.0	705	0.48E-03	108	23.0	25.0	30.0	850	0.20E-03	176	46.0	44.0	54.0	925	0.12E-03
40	18.0	22.0	34.0	727	0.26E-03	109	26.0	28.0	34.0	600	0.70E-03	177	47.0	46.0	45.0	1050	0.16E-02
41	34.0	37.0	60.0	561	0.13E-02	110	25.0	29.0	34.0	600	0.96E-03	178	43.0	40.0	50.0	1220	0.82E-03
42	30.0	38.0	50.0	485	0.14E-02	111	27.0	28.0	34.0	600	0.74E-03	179	48.0	40.0	54.0	1325	0.58E-03
43	27.0	32.0	39.0	1111	0.34E-03	112	25.0	29.0	39.0	400	0.14E-02	180	40.0	43.0	55.0	795	0.58E-03
44	30.0	34.0	45.0	484	0.12E-02	113	23.0	29.0	43.0	500	0.50E-03	181	39.5	43.5	45.0	950	0.12E-02
45	26.0	27.0	42.0	703	0.46E-03	114	27.0	30.0	35.0	700	0.68E-03	182	28.5	30.0	38.0	1010	0.15E-02
46	25.0	29.0	39.0	954	0.32E-03	115	26.0	29.0	35.0	730	0.72E-03	183	41.0	43.0	45.0	778	0.26E-03
47	27.0	30.0	50.0	1068	0.46E-03	116	25.0	28.0	45.0	925	0.44E-03	184	34.0	37.0	37.0	914	0.58E-03
48	27.0	30.0	37.0	924	0.40E-03	117	18.0	21.0	28.0	760	0.20E-03	185	30.0	33.0	38.5	900	0.60E-03
49	30.0	33.0	39.0	788	0.62E-03	118	28.0	27.0	45.0	625	0.56E-03	186	31.0	34.5	44.5	905	0.56E-03
50	30.0	38.0	53.0	481	0.92E-03	119	22.0	27.0	29.0	1075	0.30E-03	187	45.5	45.0	50.5	615	0.56E-03
51	29.0	30.0	53.0	707	0.58E-03	120	23.0	26.0	34.0	985	0.32E-03	188	38.5	42.0	54.5	730	0.50E-03
52	32.0	30.0	40.0	569	0.98E-03	121	25.0	29.0	45.0	825	0.58E-03	189	25.0	29.0	42.0	950	0.56E-03
53	22.0	23.0	33.0	889	0.24E-03	122	24.0	27.0	45.0	800	0.52E-03	190	33.0	33.0	42.5	890	0.16E-03
54	20.0	21.0	30.0	466	0.50E-03	123	23.0	26.0	40.0	625	0.58E-03	191	30.0	35.5	38.0	1120	0.38E-03
55	26.0	30.0	29.0	503	0.70E-03	124	25.0	28.0	40.0	880	0.52E-03	192	34.0	36.0	45.0	1140	0.72E-03
56	31.0	31.0	43.0	832	0.58E-03	125	24.0	28.0	45.0	1140	0.28E-03	193	26.5	32.0	50.0	845	0.58E-03
57	31.0	33.0	43.0	830	0.56E-03	126	20.0	24.0	40.0	1240	0.16E-03	194	27.5	32.5	44.0	925	0.13E-02
58	30.0	30.0	49.0	739	0.46E-03	127	26.0	29.0	45.0	650	0.70E-03	195	28.0	30.0	33.0	640	0.72E-03
59	28.0	30.0	39.0	616	0.68E-03	128	24.0	25.0	45.0	1260	0.22E-03	196	22.0	24.0	25.0	980	0.20E-03
60	27.5	30.0	31.0	760	0.30E-03	129	27.0	30.0	50.0	870	0.40E-03	197	31.5	34.0	31.5	900	0.96E-03
61	31.5	33.0	42.0	780	0.44E-03	130	27.0	30.0	45.0	860	0.50E-03	198	32.0	38.0	36.5	950	0.22E-03
62	30.5	32.0	37.0	910	0.38E-03	131	26.0	28.0	50.0	990	0.22E-03	199	26.0	29.0	39.0	470	0.68E-03
63	34.5	37.5	53.5	815	0.72E-03	132	31.0	34.0	50.0	890	0.68E-03	200	29.0	33.0	48.0	535	0.32E-03
64	32.0	34.0	41.0	970	0.28E-03	133	31.0	36.0	53.0	890	0.66E-03	201	30.5	31.0	35.0	650	0.14E-03
65	28.5	32.0	36.5	925	0.34E-03	134	41.0	41.0	63.0	915	0.12E-02	202	27.0	28.0	29.0	660	0.12E-02
66	35.0	36.0	59.0	790	0.70E-03	135	40.0	40.0	60.0	885	0.74E-03	203	32.0	33.5	45.0	545	0.26E-03
67	37.0	39.0	57.0	805	0.80E-03	136	35.0	38.0	55.0	880	0.13E-02	204	22.5	25.5	43.0	835	0.88E-03
68	35.0	38.0	33.5	953	0.68E-03	137	31.0	34.0	45.0	1250	0.52E-03	205	32.0	36.0	32.0	775	0.76E-03
69	38.0	40.0	63.0	710	0.12E-02							206	27.0	32.5	51.5	1280	0.94E-03

The inclination of the starting zone  $\theta$  is measured on a map as the average gradient of the uppermost 100 m of the path, vertically measured. The avalanche profiles are expressed by the equation  $y = ax^2 + bx + c$  (see Fig.1).  $H$  is defined as the height difference from the starting point to the vertex of the calculated parabola. The second derivative  $y'' = 2a$  describes the curvature, and by multiplying with  $H$  the theoretical profile is made dimensionless.  $H$  is usually different from the vertical drop  $Y$  of the avalanche.

The second derivative  $y''$  of the slope function is a shape factor. The shape of the path is essential to  $\alpha$ , and our experience is that avalanche paths that are just steep enough to trigger the avalanche, and keep it moving, must have longer runout distances (lower values of  $\alpha$ ) than steeper paths. This is the reason for introducing  $y''$  which describes the whole profile in more detail than  $\beta$ . If the slope really had been a parabola, we can derive the connection

$$\tan \beta = \sqrt{\frac{Hy''}{2}} + \frac{\tan 10^\circ}{2}$$

but the  $10^\circ$  point found on the map differs from this theoretical number.

In the present paper we discuss a classification of the avalanche paths in an attempt to obtain better accuracy in the runout calculation. As indicated by Lied and Bakkehøi (1980), a tendency was found for confined avalanches to obtain lower values of  $\alpha$  than unconfined avalanches, but it was not possible to confirm this tendency in the statistical analysis.

The avalanche paths are classified as obviously confined (47 avalanches) and obviously unconfined (77 avalanches). Classification is also performed on the basis of values of  $\beta$ ,  $y''$ ,  $H$ , and  $\theta$ . On steep slopes with high values of  $\beta$ ,  $y''$ , and  $\theta$ , avalanches tend to start with less snowfall than on gently inclined slopes. If avalanche velocity and runout is dependent on avalanche mass, a difference between steep and gently inclined paths concerning relative runout distance would be expected. As indicated by both Körner (1980) and Laatsch and others (1981), the model of Lied and Bakkehøi (1980) does not explicitly take mass dependency into consideration. A classification based on different values of  $\beta$  will implicitly consider a mass dependency.

The classification based on the above mentioned parameters is obtained in the following way:

$\beta$	$\theta$	$y''$	$H$ (m)
$< 30^\circ$	$< 40^\circ$	$< 6 \times 10^{-4}$	$< 600$
$30^\circ < \beta < 35^\circ$	$> 40^\circ$	$> 6 \times 10^{-4}$	$> 500$
$\beta > 35^\circ$	$< 50^\circ$	$> 12 \times 10^{-4}$	$> 900$
		$4 \times 10^{-4} < y'' < 12 \times 10^{-4}$	$600 < H < 900$
		$6 \times 10^{-4} < y'' < 14 \times 10^{-4}$	

2.1. Results

The regression analysis based on 206 avalanches gives the equation:

$$\alpha = 0.92 \beta - 7.9 \times 10^{-4} [H] + 2.4 \times 10^{-2} [H] y'' \theta + 0.04,$$

with  $R = 0.92$  and  $SD = 2.28^\circ$ . In this equation,  $[H]$  represents the numerical value of  $H$ . If, as an example, we choose  $\beta = 30^\circ$ ,  $\theta = 35^\circ$ ,  $H = 1\ 000$  m and  $y'' = 3 \times 10^{-4}$ , this will illustrate the importance of each term in the equation:

$$\alpha = 27.6^\circ - 0.79^\circ + 0.25^\circ + 0.04 = 27.1^\circ.$$

Introduction of more variables in the regression equation will not give a significant increase in the accuracy.  $\beta$  has a t-value (Daniel and Wood 1971: 353) of 19.0. The variable  $Hy''\theta$  has a t-value of 1.3, which is significant to the 0.10 level, while  $H$  is significant to the 0.12 level. Using  $\beta$  as the only free variable, this equation is obtained:

$\alpha = 0.96\beta - 1.4^\circ$ , with  $SD = 2.3^\circ$  and  $R = 0.92$ . This clearly demonstrates the dominating effect of  $\beta$ . The result indicates that, even if the total number of avalanches is increased, a higher accuracy in the prediction of avalanche runout by this method cannot be obtained. In the equation presented by Lied and Bakkehøi (1980)  $R = 0.95$  and  $SD = 2.3^\circ$ .

One regression equation for both confined (47 avalanches), and unconfined paths (77 avalanches) is computed. If avalanches in the confined paths (wide rupture zone and narrow track) obtain longer runout distances, this tendency should be found statistically by the regression analysis. No such tendency was found. By running the equation for the confined paths on unconfined avalanches and vice versa, it was not possible to identify any tendency for confined avalanches to obtain lower  $\alpha$  values than unconfined avalanches. The result may be partly explained by the inaccuracy in the model, but mainly by the fact that when an avalanche is forced into a confined path from a wider rupture zone, the snow masses must be compressed so that sintering and densification takes place. This process must lead to higher friction and consequently reduce the velocity increase.

Regression analysis is performed, based on a classification of  $\beta$  values. For tracks with  $\beta < 30^\circ$  we found this equation:

$$\alpha = 0.89\beta + 3.5 \times 10^{-2}\theta - 2.2 \times 10^{-4}[H] - 0.9^\circ,$$

with  $R = 0.84$  and  $SD = 1.49^\circ$ . Computed with the equation for all avalanches,  $SD = 1.51^\circ$ .

In our opinion, this is a high accuracy, and especially valuable on these gently inclined paths where differences in degrees amount to the biggest difference in metres concerning runout distance.

For  $30^\circ < \beta < 35^\circ$  the equation

$$\alpha = 1.15\beta - 2.5 \times 10^{-3}[H] - 5.9^\circ \text{ (59 avalanches)}$$

with  $R = 0.53$  and  $SD = 2.50^\circ$ , was found. The same sample computed with the equation found for all avalanches gave  $SD = 2.56^\circ$ .

Correspondingly, the equation for  $\beta > 35^\circ$  is

$$\alpha = 0.81\beta + 3.6 \times 10^{-2}[H] y'' \theta + 3.2^\circ \text{ (79 avalanches)}$$

with  $R = 0.62$  and  $SD = 2.67^\circ$ . This sample computed with the equation found for all avalanches gave  $SD = 2.69^\circ$ .

This last example of classification does not appear to increase the accuracy of the model.

A classification based on  $H$ ,  $y''$ ,  $\theta$  and  $\beta$  is presented in Table II.

These results indicate that  $\beta$  is the best scaling factor of the examined parameters. A classification based on  $\theta$  or  $y''$  does not increase the accuracy of the model.

In combination with  $\beta$ ,  $H$  seems to be an important variable. For  $H > 900$  m and  $\beta < 30^\circ$ ,  $SD = 1.02^\circ$  and  $R = 0.90$ . The equation for all the avalanches used on this sample gives  $SD = 1.07^\circ$ . This last result is of great value, because it improves the predictive accuracy for a group of avalanches where erroneous runout calculations have the greatest consequences. For an avalanche with  $H = 1\ 000$  m,  $\beta < 30^\circ$  and  $\alpha = 25^\circ$ , one standard deviation gives a possible longer horizontal reach  $\Delta l_1 = 91$  m and a possible shorter reach  $\Delta l_2 = 85$  m. The regression equation for this group is

$$\alpha = 0.94\beta + 0.035\theta - 2.6^\circ.$$

TABLE II. CLASSIFICATION BASED ON H,  $\gamma''$ ,  $\theta$ , AND  $\beta$

	Number	Standard deviation (SD)	Correlation coefficient (R)
All avalanches	212	2.4°	0.93
$\theta$ -classification:			
$\theta < 40^\circ$	103	2.0°	0.93
$\theta > 40^\circ$	109	2.6°	0.92
$\theta < 50^\circ$	181	2.3°	0.93
$\theta > 50^\circ$	31	2.7°	0.86
$\beta$ -classification:			
$\beta < 30^\circ$	73	1.5°	0.85
$30^\circ < \beta < 35^\circ$	60	2.9°	0.52
$\beta > 35^\circ$	79	2.6°	0.82
H-classification:			
$H < 600$ m	42	2.5°	0.86
$600$ m $< H < 900$ m	87	2.0°	0.94
$H > 500$ m	194	2.4°	0.93
$H > 900$ m	83	2.5°	0.93
$\gamma''$ -classification with $600$ m $< H < 900$ m:			
$\gamma'' < 6 \times 10^{-4}$	41	1.4°	0.93
$\gamma'' > 6 \times 10^{-4}$	46	2.6°	0.91
$\gamma'' > 12 \times 10^{-4}$	13	1.8°	0.89
$4 \times 10^{-4} < \gamma'' < 12 \times 10^{-4}$	53	2.1°	0.89
$6 \times 10^{-4} < \gamma'' < 14 \times 10^{-4}$	40	2.4°	0.88
$\gamma''$ -classification with $H > 900$ m:			
$\gamma'' < 6 \times 10^{-4}$	43	1.8°	0.92
$\gamma'' > 6 \times 10^{-4}$	40	2.5°	0.87
$\beta$ -classification with $600$ m $< H < 900$ m:			
$\beta < 30^\circ$	37	1.2°	0.91
$\beta > 30^\circ$	50	2.3°	0.89
$\beta$ -classification with $H > 900$ m:			
$\beta < 30^\circ$	20	0.9°	0.92
$\beta > 30^\circ$	60	2.7°	0.88

3. RUNOUT CALCULATION BASED ON A DYNAMIC MODEL

Perla and others (1980) presented a two-parameter model of snow avalanche motion expressed by the equation

$$\frac{1}{2} \frac{dv^2}{ds} = g(\sin \theta - \mu \cos \theta) - \frac{D}{M} v^2,$$

where M is the avalanche mass,  $\theta$  the slope angle,  $\mu$  the coefficient of friction, and D a coefficient of dynamic drag. The equation is solved numerically by dividing the entire avalanche path into small segments where  $\theta$  are considered to be constant in each segment. Each segment is assigned an angle  $\theta_i$ , a length  $L_i$ , a friction value  $\mu_i$ , and a mass/drag value  $(M/D)_i$ . Momentum loss is corrected at the segment transitions. Avalanche velocity is computed for each segment, progressively along the path, until the stopping position. The model was first applied on 25 avalanche paths in north-west USA. The usefulness of this model is dependent on a knowledge of the values of  $\mu$  and M/D. These values can vary within wide limits, with endless possibilities of combination, and still satisfy a given runout distance. The model presented by Voellmy (1955) is encumbered with the equivalent problem.

In a later work the same model was tested statistically on 136 extreme avalanche paths from the north-west USA and Norway (Bakkehøi and others 1981). The

range of M/D values was here related to the scale factor Y, i.e. the total vertical drop of the avalanche. M/D values  $Y/100 < M/D < 0.01Y$  were considered. By computing the corresponding values of  $\mu$  and velocity v, it was found that, for M/D values between 1 000 Y and 10 Y, both  $\mu$  and v are near constant.

Based on the general knowledge and measurements of avalanche speed (see section 6) and of assumed values of  $\mu$  in dry avalanches, it seems realistic to choose M/D values in the range  $10Y > M/D > Y/10$  (Bakkehøi and others 1981). This is still a wide range, and applied to runout calculations it means a fairly low accuracy in predicting runout distance.

4. STATISTICAL ANALYSIS OF THE DYNAMIC MODEL

The dynamic model introduced by Perla and others (1980) is applied on the sample of avalanches already described in this paper. The runout distance in terms of  $\alpha$  is computed for all the avalanche paths with different sets of values of  $\mu$  and M/D, and the avalanches are classified for different values of  $\beta$ ,  $\beta < 30^\circ$ ,  $30^\circ < \beta < 35^\circ$ ,  $\beta > 35^\circ$ . The values of  $\mu$  and M/D are computed for the most probable pairs, and the best fits are presented in Table III.

One general conclusion is that steep tracks need higher friction values than gentle tracks to obtain the best correlation. For  $\beta > 35^\circ$ ,  $\mu = 0.30$  and for  $\beta < 30^\circ$ ,  $\mu = 0.20$ , for identical values of M/DY. The standard deviation of residuals is between 3.2° and 3.8°, which is a wider deviation than found by the topographic model where the smallest values of SD with the same classification varied between 1.5° and 2.6°. The accuracy of the model seems to increase slightly, although not much, due to the classification, as SD = 3.2° for  $30^\circ < \beta < 35^\circ$ , and SD = 3.3° for  $\beta > 35^\circ$ , compared to SD = 3.5° for all paths. The best fitted pairs for all paths are  $\mu = 0.25$ , M/DY = 0.5, with R = 0.83 and SD = 3.5°.

The reason why higher friction values must be applied on steeper paths in the model may be as indicated in section 2. Avalanches in such slopes contain less mass of snow, and should thereby obtain a shorter runout distance.

5. COMBINATION OF THE TOPOGRAPHIC AND DYNAMIC MODELS

In our consulting work, we are frequently faced with the question of potential avalanche runout distance, and we therefore need to improve the accuracy of the existing models. The model presented by Voellmy (1955), and since then widely used in alpine countries is difficult to handle because the hydraulic radius R, flow height h, coefficient of friction  $\mu$ , and drag-coefficient  $\xi$  vary within wide limits. Years of experience are necessary to sort out empirically the right values of these constants which in turn can give realistic runout distances. This is clearly demonstrated by Föhn and Meister (1982), who documented that a 10% error in rupture width and slab height may cause  $\pm 100$  m difference in runout distance.

We have therefore developed the statistical method described earlier in this paper. On the basis of this, it is possible to predict the most probable extreme runout distance. This probabilistic way of handling the problem excludes most of the subjective judgement in fixing the values of the constants. By combining the topographic and dynamic models we see a possibility of increasing the accuracy of runout prediction and velocity estimates. The procedure is as follows. A given position in a potential runout zone is analyzed with regard to possible reach of avalanche debris. The profile of the avalanche path is drawn from a map with a scale 1:50 000 and with contour lines 20 m apart. The lowest part of the path is usually supplied with data from a detailed map of scale 1:5 000. A set of 10 to 20 x- and y-coordinates are sufficient to describe the profile. The  $\beta$  point is identified and  $\beta$  found. The inclination of the rupture zone is measured on the map, and the most probable vertical drop Y is evaluated

TABLE III. VALUES OF  $\mu$  AND  $(M/D)Y$  RELATED TO  $\beta$   
 ( $\bar{\alpha}$ : Mean of observed values,  $\bar{\alpha}_C$ : Mean of calculated values)

$\beta$	$\mu$	$(M/D)Y$	Standard deviation of residuals	Deviation $\bar{\alpha} - \bar{\alpha}_C$	Number of avalanches
$\beta < 30^\circ$	0.20	0.50	3.2°	-0.18°	69
$30^\circ < \beta < 35^\circ$	0.30	0.75	3.4°	0.10°	78
	0.25	0.50	3.5°	-0.03°	78
	0.25	0.75	3.4°	-1.39°	78
	0.30	0.50	3.3°	0.07°	88
$\beta > 35^\circ$	0.35	0.75	3.3°	0.66°	88
	0.30	0.75	3.3°	0.66°	88
All avalanches	0.35	1.0	3.8°	-0.1°	212
	0.30	0.75	3.6°	-0.04°	212
	0.25	0.5	3.5°	-0.15°	212

from the map also. The real profile is transformed to a parabolic function of the type  $y = ax^2 + bx + c$ , with the best fit found by the method of least squares.  $\alpha$  is then computed by the best fitted empirical equation (see section 2.1). The avalanche speed and runout distance are calculated by using the dynamic method described in section 4. Different pairs of values of  $\mu$  and  $M/D$  are preloaded in the computer program, and avalanche runout distance is calculated for the best fits depending on  $\beta$  (see Table III).

With the aid of a map and a computer, the whole procedure is easily done within half-an-hour. Central processing unit time for the calculations is less than 1 s.

6. VELOCITY MEASUREMENTS

In the work of Bakkehøi and others (1981) it is emphasized that values of the avalanche speed are needed to evaluate what regimes of  $\mu$  and  $M/D$  are applicable. Velocity measurements have been performed at the Ryggfonn avalanche at the avalanche research station of the Norges Geotekniske Institutt (NGI). The avalanche is triggered by explosives. Total vertical drop is ~1 000 m, and path length about 2 000 m. The avalanche volume ranges from the order of  $10^4$  to  $10^5$  m<sup>3</sup> snow.

We have two reports of velocity measurements from this avalanche. In the first, the avalanche volume was ~ $10^5$  m<sup>3</sup>. The air temperature was below 0°C in the entire path. The velocity profile is presented in Figure 2. In the second (Fig.3), the avalanche con-

sisted of ~ $5 \times 10^4$  m<sup>3</sup> snow. The 0°C isotherm was at 1 100 m a.s.l. Therefore, in the lowest part of the path, from ~1 000 to ~600 m a.s.l., the snow was wet. This again resulted in a marked reduction of avalanche speed in this part because of higher friction in the wet snow (velocity profile, see Figure 3). The avalanches were photographed by cine photography at three different points and the frontal speed was calculated by comparing the pictures with points in the path where  $x$  and  $y$  coordinates are known.

The interesting facts arising from these two field measurements are that maximum speed is as high as ~60 m s<sup>-1</sup> (frontal speed), and that both the avalanches obtained almost the same maximum speed despite the difference in mass. This observation gives support to the view that avalanche speed is more a function of snow quality in the path than of avalanche mass. The snow cover in the main part of the track consisted of light, dry snow in both cases. Moreover, these measurements illustrate that the computer program is applicable and makes it possible to choose a realistic regime of  $\mu$  and  $M/D$  when both velocity and stopping position of the avalanche are known. The best fitted pair of values of  $\mu$  and  $M/D$  from these measurements corresponds with the values found by the statistical analysis of the numerical model discussed in section 3.

CONCLUSION

In this work we have presented a topographical and statistical model which predicts avalanche runout distance based on four parameters. The para-

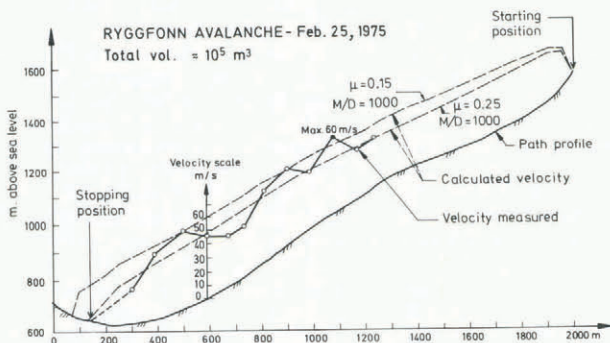


Fig.2. Velocity, measured and calculated in the Ryggfonn avalanche, February 1975.

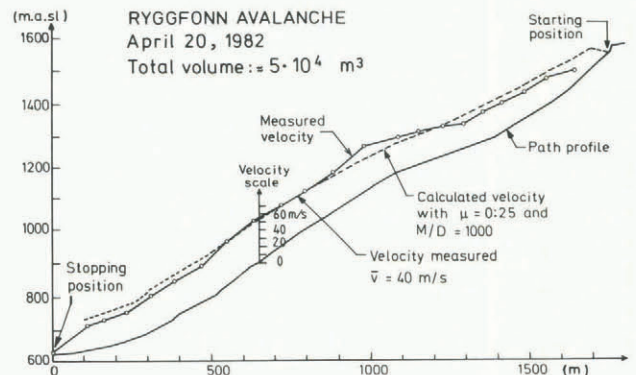


Fig.3. Velocity, measured and calculated in the Ryggfonn avalanche, April 1982.

meters are all easily measured or calculated from topographic maps. By classification of the avalanche paths we have increased the accuracy of the model. The classification of the avalanches seems to confirm that confinement of the path has no significant influence on the runout distance. The main reason for this is thought to be that compression, sintering, and density increase takes place during the confinement. These processes increase the friction and reduce the velocity increase created by the confinement. Avalanches on steep paths seem to obtain a relatively short runout distance related to  $\alpha$ . This may be caused by a relatively greater loss of energy due to the dependent friction term  $v^2$  when avalanches are running on steep slopes with high speed. In addition, steep slopes tend to contain less snow than gentle slopes when avalanches are triggered, and these avalanches therefore have less mass and volume. This again may lead to relatively lower speeds and shorter runout distance.

The results obtained by the numerical/dynamical model which is applied to avalanche population, seems to lead to the same conclusion, i.e. that avalanches on steep slopes need greater friction values to fit the observed runout distances.

By the topographical method we have obtained a prediction accuracy of  $SD \approx 1$  to  $2^\circ$  of the runout distance  $\alpha$ , depending on the path topography. This is in the order of  $\pm 100$  to  $\pm 200$  m for an avalanche with a vertical drop of 1 000 m and  $\alpha \approx 25^\circ$ . In combination with the numerical/dynamical model presented by Perla and others (1980), it is possible to predict speed and runout distance with an accuracy which is applicable for practical consulting work. To increase the accuracy of the model, measurements of speed and runout distance from full-scale experiments will be particularly important.

#### ACKNOWLEDGEMENTS

The authors wish to thank P Johnson and K Kristensen who did most of the difficult and time-consuming field and map work, and R Volden at the Norsk Regnesentral, who analyzed the statistical methods. We are also grateful to the members of the avalanche group at NGI for many stimulating discussions.

#### REFERENCES

- Bakkehoi S, Cheng T, Domaas U, Lied K, Perla R I, Schieldrop B 1981 On the computation of parameters that model snow avalanche motion. *Canadian Geotechnical Journal* 18(1): 121-130
- Buser O, Frutiger H 1980 Observed maximum run-out distance of snow avalanches and the determination of the friction coefficients  $\mu$  and  $\xi$ . *Journal of Glaciology* 26(94): 121-130
- Daniel C, Wood F 1971 *Fitting equations to data*. New York, John Wiley and Sons
- Föhn P, Meister R 1982 Determination of avalanche magnitude and frequency by direct observations and/or with the aid of indirect snowcover data. *Mitteilungen der Forstlichen Bundesversuchsanstalt Wien* 144: 207-228
- Körner H J 1980 Modelle zur Berechnung der Bergsturz- und Lawinenbewegung. *Interpraevent* 1980 Band 2: 15-55
- Laatsch W, Zenke B, Dankerl J 1981 Verfahren zur Reichweiten- und Stossdruckberechnung von Fliesslawinen. *Schriftenreihe der Forstwissenschaftlichen Fakultät der Universität München und der Bayerischen Forstlichen Versuchs- und Forschungsanstalt* 47
- Lied K, Bakkehoi S 1980 Empirical calculations of snow-avalanche run-out distance based on topographic parameters. *Journal of Glaciology* 26(94): 165-177
- Perla R, Cheng T T, McClung D M 1980 A two parameter model of snow avalanche motion. *Journal of Glaciology* 26(94): 197-207

- Quervain M R de 1972 Lawinenbildung. In Castelberg F and 4 others (eds) *Lawinenschutz in der Schweiz. Bündnerwald. Zeitschrift des Bündnerischen Forstvereins und der SELVA, Genossenschaft der Bündnerischen Holzproduzenten*, Beiheft 9: 15-32
- Voellmy A 1955 Über die Zerstörungskraft von Lawinen. *Schweizerische Bauzeitung* 73(12): 159-162 (15): 212-217 (17): 246-249 (19): 280-285